Available online at www.sciencedirect.com
SCIENCE DIRECT
Bioorganic & Medicinal Chemistry 14 (2006) 2627–2635
Bioorganic & Medicinal Chemistry

New leads of metallo-β-lactamase inhibitors from structure-based pharmacophore design

Lars Olsen,[a,*] Sandra Jost,[b] Hans-Werner Adolph,[c] Ingrid Pettersson,[d] Lars Hemmingsen[e] and Flemming S. Jørgensen[a]

[a]*Biostructural Research, Department of Medicinal Chemistry, Danish University of Pharmaceutical Sciences, Universitetsparken 2, DK-2100 København, Denmark*
[b]*Biochemistry and Organic Chemistry, Universtity of the Saarland, D-66041 Saarbrücken, Germany*
[c]*Organic Macromolecular Chemistry and Center for Bioinformatics, University of the Saarland, D-66041 Saarbrücken, Germany*
[d]*Structure and Biophysical Chemistry, Novo Nordisk A/S, Novo Nordisk Park, DK-2760 Måløv, Denmark*
[e]*Department of Natural Science, The Royal Veterinary and Agricultural University, Thorvaldsensvej 40, DK-1871 Frederiksberg C, Denmark*

Received 22 August 2005; revised 16 November 2005; accepted 22 November 2005
Available online 27 December 2005

Abstract—We have applied pharmacophore generation, database searching, docking methodologies, and experimental enzyme kinetics to discover new structures for design of di-zinc metallo-β-lactamase inhibitors. Based on crystal structures of class B1 metallo-β-lactamases with a succinic acid and a mercapto-carboxylic acid inhibitor bound to the enzyme, two pharmacophore models were constructed. With the Catalyst program, these pharmacophores were used to search the ACD database, which provided a total of 74 hits representing four different chemical classes of compounds: Dicarboxylic acids, phosphonic and sulfonic acid derivatives, and mercapto-carboxylic acids. All hits were docked into different metallo-β-lactamases (from classes B1 and B3) using the GOLD docking program. A selection scheme based on the GOLD scores, the Catalyst fit and shape values, and the size of the compounds (molecular weight, surface area, and number of rotatable bonds) was developed and thirteen compounds representing all four chemical classes were selected for experimental studies. Three compounds with new scaffolds hitherto not present in metallo-β-lactamase inhibitors have IC_{50} values less than 15 μM and may serve as starting points in the design of metallo-β-lactamase inhibitors.

1. Introduction

One of the major mechanisms underlying bacterial resistance is the production of β-lactamases which are enzymes capable of hydrolyzing β-lactam-containing antibiotics such as penicillins. β-Lactamases have been divided into four classes, A–D,[1] where classes A, C, and D contain a serine in the active site that is involved in catalysis, and class B are the so-called metallo-β-lactamases (MBLs) that require metal ions for catalytic activity. The MBLs hydrolyze a broad spectrum of lactam-antibiotics, and in contrast to the serine-β-lactamases carbapenems are also cleaved.

The MBLs have been divided into subclasses B1–B3 based on their amino acid sequences.[2,3] Crystal structures have been determined for the subclass B1 enzymes from *Bacillus cereus* (BCII), *Bacteroides fragilis* (CcrA), *Pseudomonas aeruginosa* (IMP-1), and *Chryseobacterium meningosepticum* (BlaB),[4–15] *Aeromonas hydrophila* (CphA) from subclass B2,[16] and *Stenotrophomonas maltophilia* (L1) and *Fluoribacter gormanii* (FEZ-1) for the subclass B3 enzyme.[17,18] They have revealed that two metal ions may be bound, with a water molecule bridging them, which is likely to perform a nucleophilic attack on the lactam ring. Some of the MBLs can, however, also function as mononuclear enzymes.[19] The present views on the roles of metal ion(s) in metallo-β-lactamases and a possibly variable metal ion content under physiological conditions have been reviewed recently.[20]

Various types of MBL inhibitors of subclasses B1–B3 have been reported in the literature, for example, trifluoromethyl alcohols and ketones,[21] biphenyl tetrazoles,[13]

Keywords: Bacterial resistance; Metallo-β-lactamase; Inhibitors design; Structure-based pharmacophore.
* Corresponding author. Tel.: +45 35 30 63 05; fax: +45 35 30 60 40; e-mail: lo@dfuni.dk

0968-0896/$ - see front matter © 2005 Elsevier Ltd. All rights reserved.
doi:10.1016/j.bmc.2005.11.046

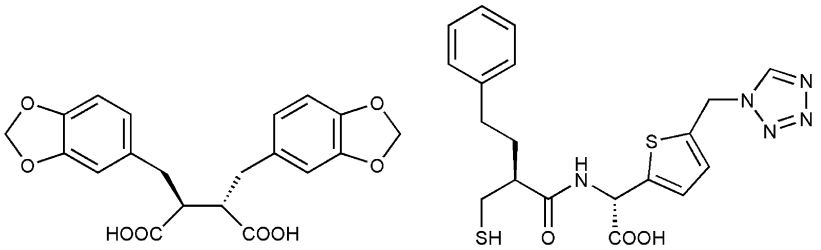

PDB: 1JJT PDB: 1DD6

Figure 1. Inhibitors co-crystallized with IMP-1 (PDB codes 1JJT[14] and 1DD6[8]).

β-lactams as carbapenem derivatives,[22] cephamycins, moxalactam,[23] and 6-methylidene penems,[24] hydroxamic acids,[25] thiols,[26–28] peptides,[29,30] thioesters,[26,28,31] mercapto-carboxylates,[8,26,27,32] 2,3-disubstituted succinic acids,[14] tricyclic natural compounds,[12] and sulfonylhydrazones.[33] In particular, the 2,3-disubstituted succinic acids[14] and mercapto-carboxylic inhibitors[8,26] are potent inhibitors with inhibition constants in the 3–90 nM-range.

Structures of MBL–inhibitor complexes have been solved for some of the most potent types of inhibitors, two of the 2,3-disubstituted succinic acids (PDB codes: 1JJT and 1JJE)[14] and the mercapto-carboxylic acid inhibitors (PDB code: 1DD6)[8] (Fig. 1). The 2,3-disubstituted succinic acids bind to IMP-1 (Fig. 2) with the carboxylate groups coordinating to the zinc ions, Lys224 and Asn233 (the amino acids are numbered according to the standard numbering scheme throughout the paper[2,3]), whereas the aromatic substituents interact with the hydrophobic amino acid residues in a flexible flab of the enzyme. The mercapto-carboxylic acid compound (Fig. 1)[8] binds with its sulfur bridging the two zinc ions, whereas the carboxylate and the hydrophobic parts of the inhibitor bind in the same manner as reported for the succinic acid inhibitors. Complexes for the CcrA enzyme have also been solved with MES (1A7T),[10] a biphenyl tetrazole (1A8T),[13] and tricyclic carboxylic acid (1KR3).[12] The two latter studies show that mainly the zinc ion site, in which an Asp, a Cys, and a His coordinate to the zinc ion, is involved in the binding of the inhibitor.

Although a number of inhibitors have been reported, none of them have been developed into drugs. This work aims at identifying new structures which may serve as new leads for MBL inhibitors. The work includes pharmacophore generation, database searching and docking methodologies, and subsequent experimental determinations.

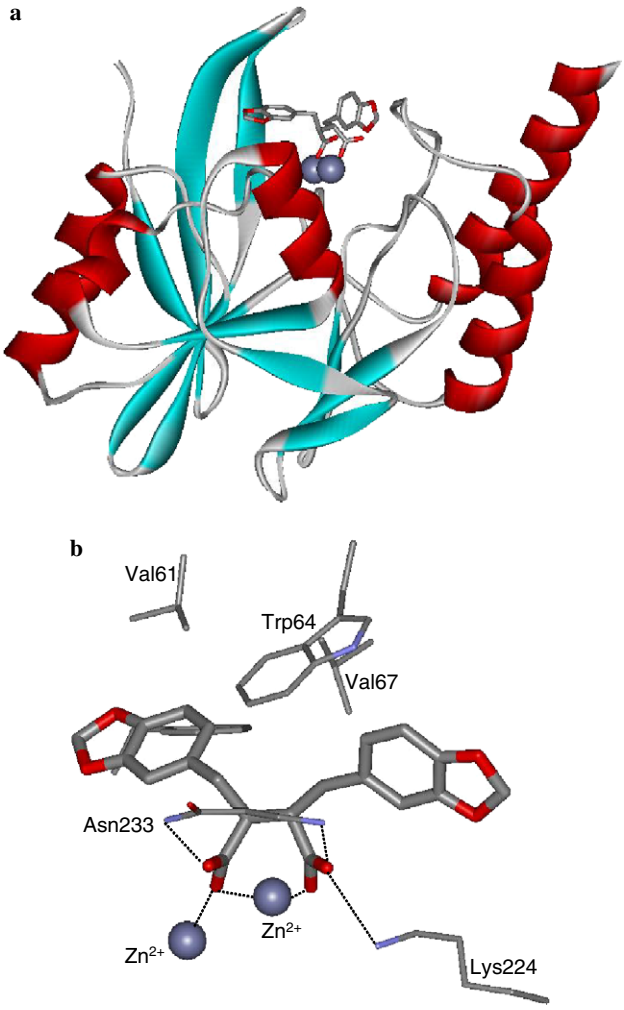

Figure 2. (a) A succinic acid inhibitor in complex with IMP-1 (PDB code 1JJT).[14] (b) Enzyme–ligand contacts for IMP-1 (PDB code 1JJT).[14] The amino acids are numbered according to Galleni et al.[2]

2. Results and discussion

2.1. Database search and characterization of the hits

The succinic acid and mercapto-carboxylic acid inhibitors, that are shown in Figure 1, have been co-crystallized with the IMP-1 enzyme and are currently some of the most potent known MBL inhibitors. Three 3D pharmacophores were generated from the crystallized ligands (Figs. 9 and 10) and ACD searched for compounds mapping to the pharmacophores. This resulted in 68 and 31 hits for the pharmacophores generated from the inhibitor crystallized in the 1JJT and 1DD6 structures, respectively, of which 25 were identical. Thus, 74 hits in total were obtained from the database searches.

To characterize the hits, descriptors were calculated, that are related to: size (surface areas and molecular

weight) and flexibility (number of rotatable bonds) of the compound, and how well they fit the pharmacophoric elements (Catalyst fit and shape values) and into the enzyme (GOLD score). The reason for taking the size of the compound into consideration is that the affinity or other properties subsequently can be optimized by introducing other chemical groups without ending up with too large a compound. Restricted flexibility of the compound is advantageous with respect to binding affinity, since it will only lose little entropy when being bound to the enzyme. To determine how well the compound fits into the active site of the enzyme, the GOLD score was used, because it can be correlated to the MBL affinity within different chemical classes with respect to the metal ion binding group.[34]

The descriptors of the hits were analyzed using PCA. Enzyme–compound complexes with high GOLD scores are found in the lower right part of the loadings plot (Fig. 3a), whereas compounds that fit the defined pharmacophoric features are in the upper right part. Small compounds can be found in the right part of the plot, since the descriptors that are related to size (molecular weight and surface area) are in the left part of the loadings plot.

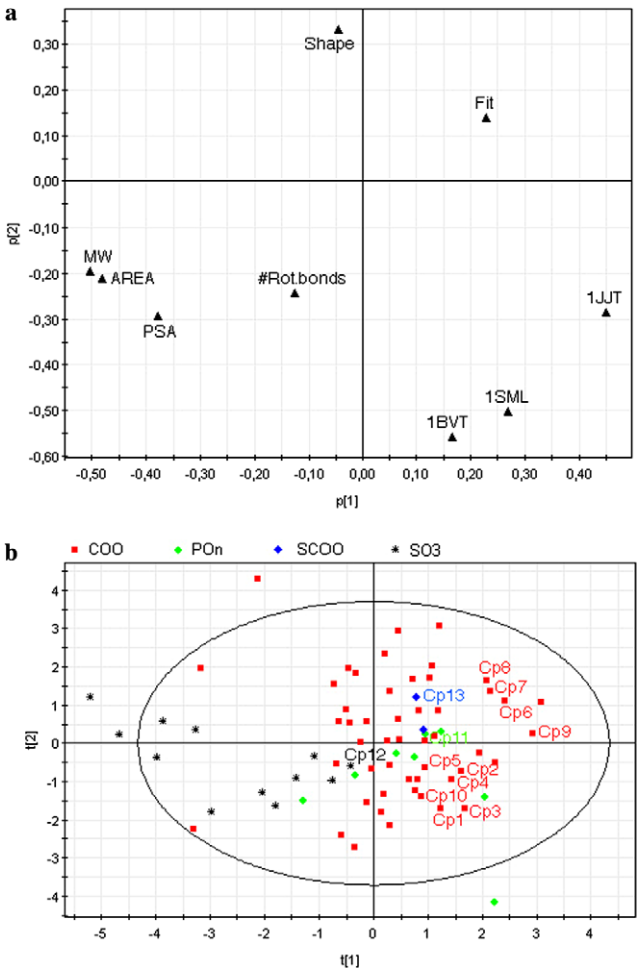

Figure 3. (a) Loadings plot from the principal component analysis of the molecular descriptors. Fit, catalyst fit value; shape, catalyst shape value; 1JJT/1BVT/1SML, GOLD score when docked into 1JJT/1BVT/1SML, # rot bonds, number of rotatable bonds; Mw, molecular weight; AREA, non-polar surface area; PSA, polar surface area. (b) Score plot from the principal component analysis. The following abbreviations are used for ligands containing carboxylic acid groups, COO; phosphonic acid derivatives, PO*n*; mercapto-carboxylates: SCOO; sulfonic acid derivatives SO_3.

Most of the hits contain carboxylic acids (mainly dicarboxylic acids) and Figure 3b shows that most of them are located in the right part of the PCA plot, indicating that they may have a high GOLD score, are small, or fit the pharmacophoric elements well. Most of the sulfonic acid derivatives are further to the left in the score plot, which indicates that they generally are larger in size, fit the pharmacophore less well, or that the GOLD score is lower.

2.2. Selection of compounds for experimental testing

Based on the PCA (loadings plot, Fig. 3a), compounds found in the blue triangle in Figure 4 would in general be relatively small and have reduced flexibility, fit the pharmacophoric elements, and have good enzyme–ligand contacts. Thus, hits in that region with different metal ion binding groups were selected for experimental determinations of the IC_{50} values.

The selected compounds are shown in Figure 5, and descriptors used to characterize them are given in Table 1. All these compounds, except for compound **XII**, are found to the right in the score plot. Most of the selected compounds are dicarboxylic acids, that are either clustered in the lower right (compounds **I**–**V**, **X**) or in the upper right part (compounds **VI**–**IX**) of the score plot. Compounds **I**–**V** and **X** have many flexible bonds (8–10), are generally of moderate molecular weight (350–400), and have GOLD scores of around 70–95. Compounds **VI**–**IX** are relatively small (molecular weight less than 320), have few rotatable bonds (4–6) and fit the pharmacophore well (fit value of 3.6–3.8).

The only selected compound found to the left of the center in the score plot is a sulfonic acid derivative

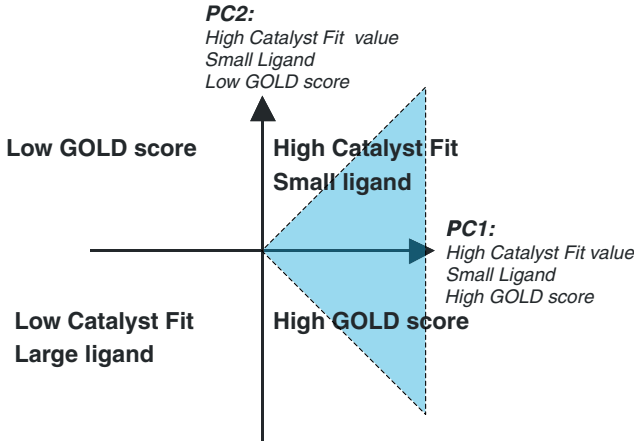

Figure 4. Schematic drawing of the score plot with the first principal component (PC) plotted against the second one. Regions in the score plot, that was used to select compounds for experimental determinations of the IC_{50} value, are colored blue.

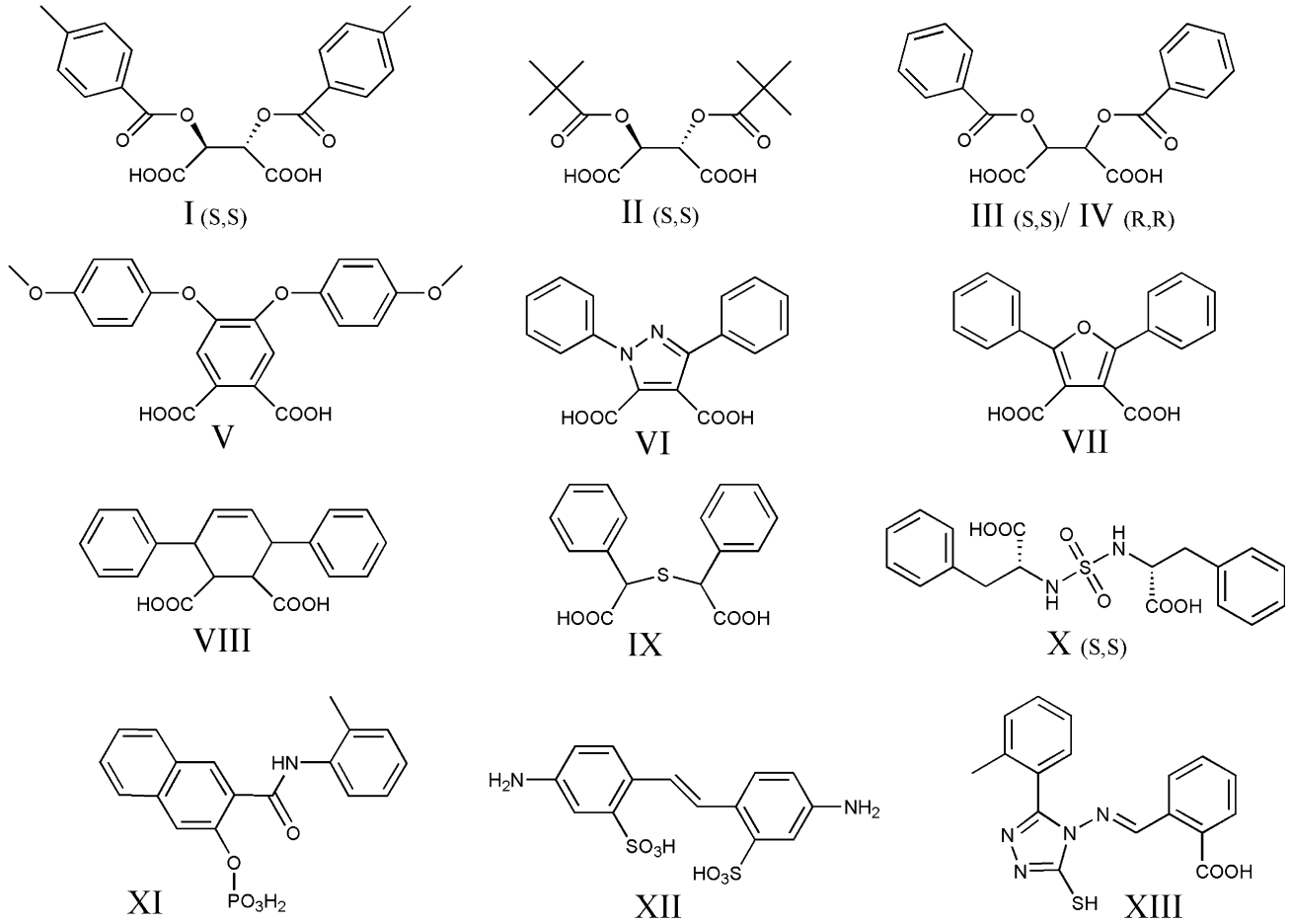

Figure 5. Compounds selected for experimental determinations of the IC_{50} value.

Table 1. Molecular descriptors of the compounds that were selected for experimental determination of the IC_{50} value

Compound[a]	Database search		GOLD scores[e]			Molecular size			
	Fit[c]	Shape[d]	BCII	IMP-1	L1	# Rot bonds[f]	Mw[g]	AREA[h]	PSA[i]
I	2.20	0.58	79	96	85	9	384	642	178
II	0.30	0.54	70	96	73	9	316	544	160
III[b]	1.44	0.53	93	97	82	9	356	579	178
IV	2.18	0.55	74	93	70	9	356	579	178
V[b]	2.63	0.61	66	91	81	8	408	649	210
VI	3.58	0.60	64	87	65	4	306	499	164
VII	3.72	0.63	66	87	66	4	306	517	173
VIII	3.72	0.70	63	90	47	4	320	660	136
IX	3.76	0.61	73	88	75	6	300	503	133
X	2.60	0.63	82	81	81	10	390	627	187
XI	3.24	0.64	72	74	68	4	368	606	167
XII	0.56	0.53	67	74	64	5	369	565	358
XIII[b]	3.47	0.54	66	50	79	4	336	565	190

[a] Compounds selected for experimental determination.
[b] The pharmacophore was generated from the mercapto-carboxylate inhibitor that is co-crystallized in IMP-1 (PDB code 1DD6). All other hits were obtained from the search with the pharmacophore generated from the succinic acid that is co-crystallized in IMP-1 (PDB code 1JJT).
[c] Catalyst fit value.
[d] Catalyst shape value.
[e] Gold score when docked into BCII/IMP-1/L1.
[f] Number of rotatable bonds.
[g] Molecular weight.
[h] Non-polar surface area in $Å^2$.
[i] PSA, polar surface area $Å^2$.

(compound **XII**). It has, however, the most positive first principal component contribution of this class of compounds, indicating that it has some of the desired properties.

2.3. Analysis of active compounds

The pharmacophores were developed on the basis of two potent inhibitors (Fig. 1) crystallized with the di-zinc IMP-1 enzyme. Accordingly, the experimental testing and docking of the compounds into the enzymes was performed for the di-zinc BCII and L1 enzymes. The BCII enzyme functions with either one or two zinc ions present,[35] but by considering the di-zinc enzyme, the problems associated with which metal site, that is occupied for the mono-zinc species, can be avoided.[36] Furthermore, inhibition of subclass B1 and B3 enzymes is usually determined under di-zinc conditions. Thus, we have worked with the di-zinc enzyme to obtain data which are comparable with other published data.

Among the 13 tested hits, compounds **VI**, **VII**, and **XIII** are inhibitors with IC_{50} values in the 10–100 μM range, see Table 2. Due to strong absorbance in the same UV region as the substrate, it was not possible to use higher concentrations of compound **XI**. The other compounds all have IC_{50} values that are larger than 100 μM. For most of the compounds, a lower limit and not the exact IC_{50} value was determined.

As mentioned earlier, there are two clusters in the score plot from the PCA for the dicarboxylic acid compounds (Fig. 3b). Both clusters contain compounds that have high GOLD scores when docked into the enzyme, and they mainly differ in the size and number of rotatable bonds. Interestingly, the two carboxylic acid-containing hits that are inhibitors (compounds **VI** and **VII**) are both found in the cluster in the upper right part of the score plot, whereas none of the compounds in the other cluster of compounds showed inhibition.

Table 2. IC_{50} values (in μM)[a]

Compound	BCII	L1
I	>1000	>1000
II	>500	>500
III	>1500	>50,000
IV	>1000	>1000
V	>100	>100
VI	14	150
VII	7	30
VIII	1000	250
IX	2500	300
X	>2500	>1000
XI	>40	>200
XII	>100	>100
XIII	100	15

[a] For many of the compounds, IC_{50} values are given as lower limits, because the maximum concentration applicable for inhibition studies was limited, either due to limited solubility or strong light absorption in the range used to follow substrate hydrolysis. In all cases, some inhibition was observed, but the investigated concentration range did not allow extrapolation to precise numerical IC_{50} values. The IC_{50} values have a standard deviation of 20–30%.

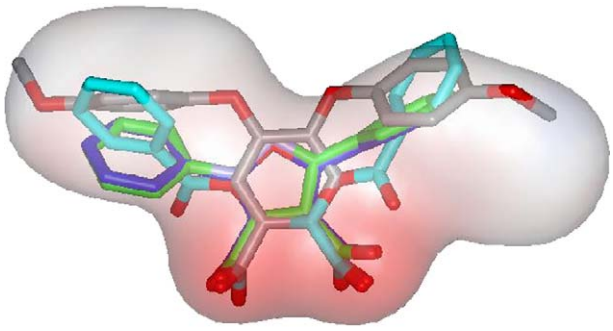

Figure 6. Compounds **III** (C atoms cyan), **V** (C atoms grey), **VI** (C atoms green), and **VII** (C atoms blue) in the orientation when docked into IMP-1. The electrostatic surface of the succinic acid inhibitor that was crystallized with the enzyme (see Fig. 1) is also shown.

Figure 6 shows two compounds from each cluster, compounds **III** and **V** from the lower, and **VI** and **VII** from the upper parts of the PCA plot, in the orientation when docked into the IMP-1 enzyme. The binding modes in BCII and IMP-1 are very similar. The high GOLD scores indicate that these compounds fit well into the enzyme. The dockings reveal that their binding modes are similar to those of the succinic acids crystallized with IMP-1.[14] The two carboxylate groups coordinate to the zinc ions and the aromatic groups bind in hydrophobic regions of the enzyme. Compounds **III** and **V** clearly occupy more space in the cavity than **VI** and **VII**, but not more than the inhibitor that was crystallized with the enzyme (the electrostatic surface of this inhibitor shown in the figure). The fact that the GOLD scores are high for all compounds also indicates that there is space enough for **III** and **V**. However, compounds **III** and **V** differ from **VI** and **VII** in the polarity and flexibility of the ligand, as also indicated by their presence in the other cluster of carboxylic acid-containing compounds. In contrast to compounds **VI** and **VII**, compound **III** contains two carbonyl oxygen atoms, and a further inspection of docked structures reveals that there are no hydrogen bonds between the carbonyl oxygen atoms in the ester groups and the enzyme, which clearly is unfavorable. This is probably also the reason why compounds **I**, **II**, **IV**, **X**, and **XII** have high GOLD scores but experimentally demonstrate only weak binding. Compound **V** has more rotatable bonds than **VI** and **VII**, and will therefore lose more entropy when binding to the enzyme, which is also clearly unfavorable for binding.

Since there is no penalty in the GOLD score for missing hydrogen bonds between the ligand and enzyme, considering only GOLD in the selection process may result in too many false positives. In addition, loss of entropy when the ligand is binding to the enzyme is not included in the GOLD scoring function, and therefore it is necessary to consider the same when selecting ligands for experimental testing. These effects contribute to placing two of the dicarboxylic acid inhibitors in the cluster of compounds in the upper part of the PCA plot.

Figures 7 and 8 show the docked structures of compound **VII** bound to BCII and compound **XIII** bound

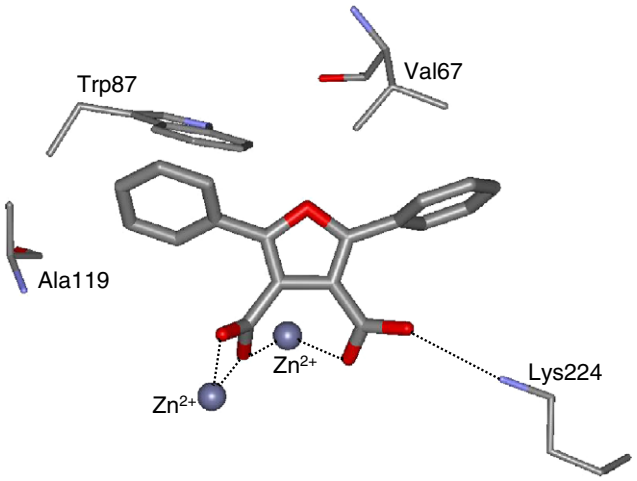

Figure 7. Compound **VII** docked into the MBL from BCII (1BVT) with the GOLD program.

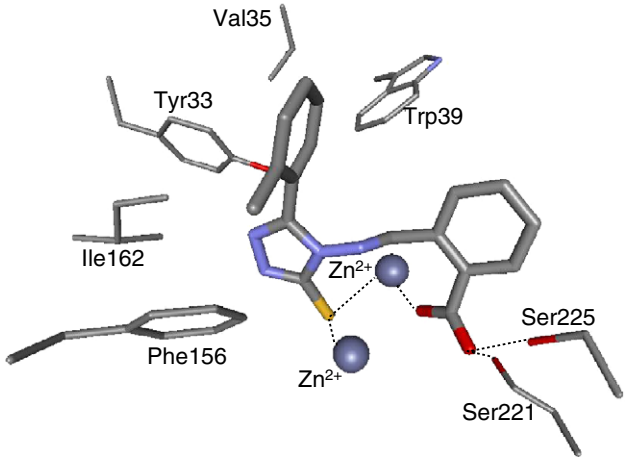

Figure 8. Compound **XIII** docked into the MBL from L1 (1SML) with the GOLD program.

to the L1 enzyme. The phenyl groups of compound **VII** make favorable hydrophobic interactions with Val67, Ala119, and Trp87 in BCII. The carboxylate groups bind to the zinc ions and to Lys224. Since compound **VI** is very similar to **VII**, the docked structures have similar binding modes. It is notable that there is a 10-fold difference in the IC_{50} value between compound **VI** bound to BCII compared to that L1. Although being similar to bound succinic acids, this scaffold with the carboxylic acid groups directly attached to a five-membered hetero-cyclic aromatic ring is, to our knowledge, new.

Dockings of compound **XIII** into L1 suggest that it binds with the sulfur bridging the two metal ions and the carboxylate group to the zinc ion and two serines (Ser221 and Ser225). The aromatic rings interact with hydrophobic groups (Tyr33, Val35, Trp39, Phe156, and Ile162) in the enzyme. Such binding mode of a mercapto group has previously been suggested based on spectroscopic[37] and docking studies,[38] and observed in the 1DD6 crystal structure.[8] The methyl group on one of the aromatic groups points directly toward Phe156. Compound **XIII** was identified from the database search using a pharmacophore that was generated from the ligand which is crystallized with IMP-1 (1DD6). In contrast to most of the other selected compounds that were identified in the other database search, it is not symmetric as a result of the pharmacophore not being symmetric. This type of inhibitor also contains a new scaffold compared to other known MBL inhibitors. Interestingly, compound **XIII** is a good inhibitor of the L1 enzyme. Only few inhibitors of this enzyme have been reported previously in the literature,[8,26,28,30] one of them being the mercapto-carboxylic acid inhibitor that was used to generate one of the pharmacophores (IC_{50} around 0.5 μM).[8]

3. Conclusion

In this work, we have applied pharmacophore generation, database searching, and docking methodologies, and subsequently experimental enzyme kinetics, to discover new structures which could be further optimized as inhibitors of di-zinc MBLs. From the database search, 74 hits were obtained and the inhibitory effect was tested for 13 of these compounds.

We used different criteria to select compounds for experimental determinations of the IC_{50} value: They should: (1) fit into the active site of the enzyme (judged from the score in a GOLD docking), (2) fit the pharmacophoric elements (Catalyst fit and shape values), and (3) be relatively small (molecular weight, surface area, and number of rotatable bonds). In addition, they should (4) contain different types of potential metal binding groups. The experimental IC_{50} values showed that in most cases this way of selecting ligands worked reasonably well. However, the GOLD score alone should be used with caution, because there is no penalty for missing hydrogen bonds between the ligand and the protein, which gives too many false positives.

Three of the tested compounds were new inhibitors of the BCII and L1 MBLs, with IC_{50} values in the 10–100 μM range. The three new inhibitors have new scaffolds—two of them have two carboxylic acid groups bound to a pyrazole or furan ring, whereas the third inhibitor contains a mercapto-carboxylic acid group.

4. Materials and methods

4.1. Docking with the GOLD program

The GOLD program (version 1.2) was used for the dockings.[39] In GOLD, metal ions are considered to bind to hydrogen bond acceptors in the ligand. Coordination points are added at points around the metal, where coordination sites are missing. These coordination points can then bind to acceptor atoms in the ligand. The capability of GOLD to study ligand binding to metallo-β-lactamases has previously been evaluated and showed that the binding, and in particular the direct

coordination to the zinc ions, corresponded very well with those determined experimentally.[34]

The ligands from the database search were docked into BCII, IMP-1, and L1 using the X-ray structures, 1BVT,[4] 1JJT,[14] and 1SML,[18] respectively. All water molecules and ligands were removed from the proteins. The binding site of the ligands was defined as a 15 Å sphere centered at the zinc ion that is coordinated by Asp, Cys, and His for BCII and IMP-1, and Asp and two His for L1. Peptide bonds in the ligands were allowed to flip between a cis or trans conformation. Otherwise, default settings were applied.

4.2. Database search using Catalyst

Catalyst (version 4.6) was used for mapping pharmacophore features and for database searching.[40–45] The features were mapped with the tolerance value equal to 1.5 Å. Search through the Available Chemicals Database (ACD) was performed with the fast flexible search method. One pharmacophore model was generated based on the succinic acid crystallized with IMP-1 (PDB code: 1JJT),[14] Figure 9. In this pharmacophore model, the carboxylic acid groups were mapped as negatively ionizable features and the phenyl rings were mapped as hydrophobic features. Two pharmacophore models were generated for a mecapto-carboxylate ligand crystallized with IMP-1[8] (PDB code: 1DD6), see Figure 10. The carboxylic acid was mapped as a negatively ionizable feature, the mercapto group as a hydrogen bonding acceptor feature, and the thiophene ring and the phenyl ring as hydrophobic features. Since a mercapto group is not regarded as a negatively ionizable group in Catalyst, it was mapped as a hydrogen bond accepting feature with two different directions. A shape constraint (0.7/1.3 Å as minimum/maximum) was added to all three pharmacophore models.

4.3. Descriptors and multivariate data analysis

Descriptors were calculated and used in a principal component analysis (PCA). The following descriptors were determined using Sybyl:[46] molecular weight, polar and non-polar surface areas, and a number of rotatable bonds (defined as a single bond, not in a ring, where the terminal atoms have at least one substituent). In addition, the GOLD score from the docking of the ligands, and the Catalyst shape and Fit values from the Catalyst search were used as descriptors.

The multivariate data analysis was performed using Simca-P, version 10.0.[47] A two-component model was obtained that explained 58% of the variance in the data, with the first principal component explaining 33%.

4.4. Experimentals

All kinetic measurements were performed at 25 °C in 15 mM HEPES (Fluka), pH 7.0. The buffer contained 100 μM additional zinc (Fluka). As a substrate the antibiotic Imipenem (a kind gift of Merck Sharp and Dohme, Rahway, NY, USA) was used, following the hydrolysis at 300 nm ($\Delta\varepsilon$ (300 nm) = $-9000\ M^{-1}\ cm^{-1}$). A UV/VIS spectrophotometer (Perkin & Elmer, Überlingen, Germany) was used to monitor the change in absorbance. The imipenem concentration was 70 μM in experiments with L1 and 150 μM with BCII, respectively. The IC_{50} values were determined from initial rates by variation of the inhibitor concentration in the range of the respective value. Standard non-linear regression analysis was used for data evaluation:

$$f = y_0 + \frac{a}{\left(1 + \frac{[I]}{IC_{50}}\right)^c},$$

where f is the remaining activity at a given concentration [I] of the inhibitor; y_0 is the remaining activity under complete inhibition; $y_0 + a$ is the non-inhibited velocity; c the exponent with value 1 in case of competitive inhibition. It was verified that the inhibitors were competitive. The IC_{50} values have a standard deviation of 20–30%. For many of the compounds, IC_{50} values are given as lower limits. For these compounds, the maximum concentration applicable for inhibition studies was limited. Either the substances possess a limited solubility or they show strong light absorption in the range used to follow substrate hydrolysis. In all cases, some inhibition was observed but the investigated concentration range did not allow extrapolation to precise numerical IC_{50} values.

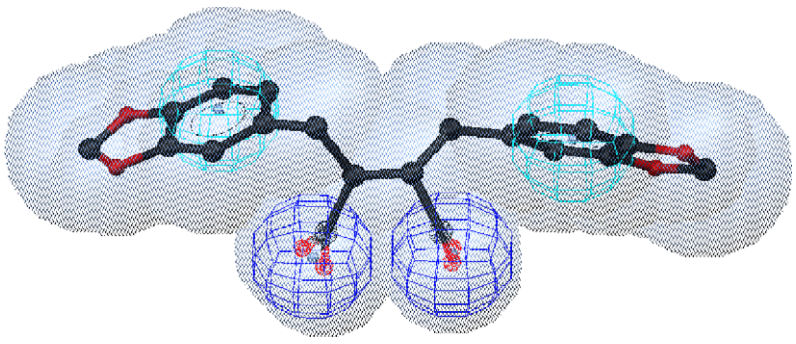

Figure 9. Pharmacophore generated from the succinic acid inhibitor crystallized in IMP-1 (PDB code 1JJT). The shaded part that surrounds the molecule shows the shape, whereas the light/dark spheres show the hydrophobic/negative features.

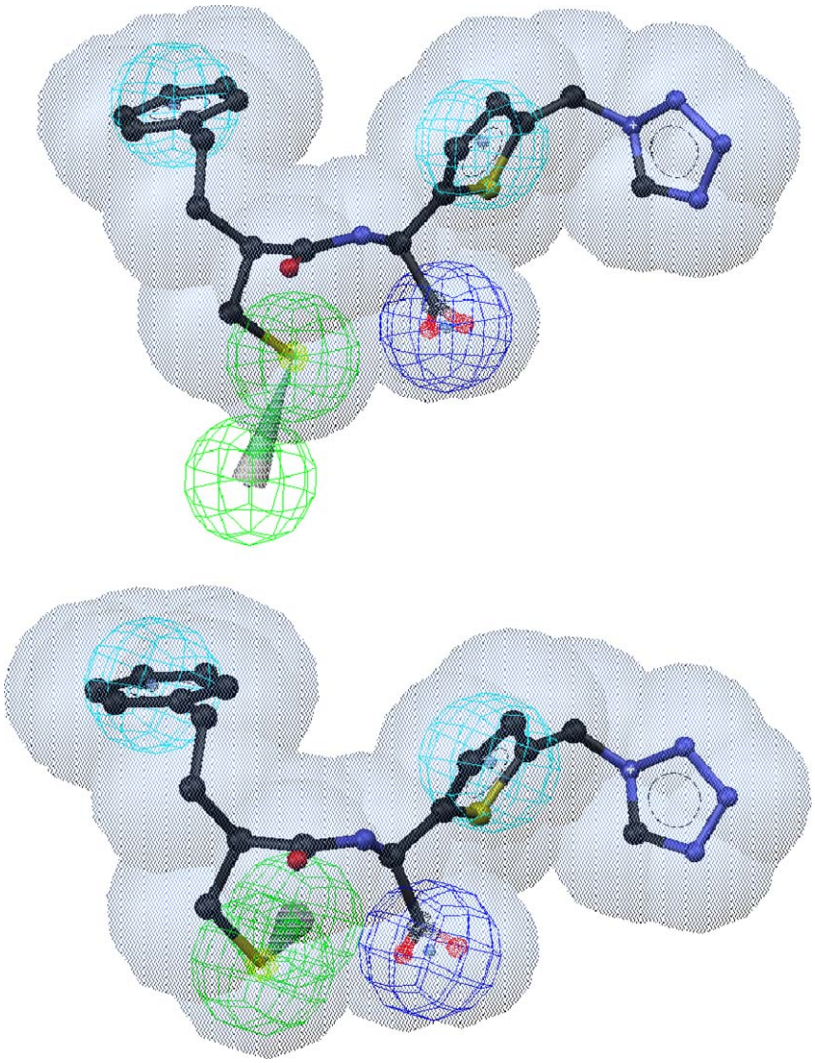

Figure 10. Pharmacophore generated from the mercapto-carboxylic acid inhibitor crystallized in IMP-1 (PDB code 1DD6). The shaded part that surrounds the molecule shows the shape, whereas the light/dark spheres show the hydrophobic/negative features. The green spheres show hydrogen-bonding acceptor features.

Thirteen compounds were purchased (the ACD name given in parentheses). **I** Di-*p*-toluoyl-D-tartaric acid hydrate (MFCD00149567) from Aldrich; **II** Dipivaloyl-D-tartaric acid (MFCD00015634) from Aldrich; **III** dibenzoyl-D-tartaric acid-monohydrate (MFCD00150722) from Lancaster; **IV** dibenzoyl-L-tartaric acid-monohydrate (MFCD00003074) from ABCR; **V** 4,5-di-(4-methoxy-phenoxy)-phthalic acid (MFCD00832097) from Maybridge; **VI** 2,5-diphenyl-2*H*-pyrazol-3,4-dicarboxylic acid (MFCD00475539) from Sigma–Aldrich; **VII** 2.5-diphenyl-3,4-furandicarboxylic acid (MFCD00666877) from SPECS; **VIII** 1,4-diphenylcyclohex-2-en-5,6-dicarboxylic acid (MFCD00181247) from Sigma–Aldrich; **IX** diphenyl-acetic acid-sulfide (MFCD00666788) from Sigma–Aldrich; **X** (S;S)-*N*,*N*′-(1,1′-bishydroxycarbonyl-2,2′-diphenyl)- diethyl-sulfonyldiamide (MFCD01850914) from Rare Chemicals; **XI** naphthol-as-mx-phosphate (MFCD00150898) from Fluka; **XII** 4,4′-diaminostilbene-2,2′-disulfonic acid (MFCD00024946) from ABCR; **XIII** 2-(((3-mercapto-5-(2-methylphenyl)-4*H*-1,2,4-triazol-4-yl) imino)me)benzoic acid (MFCD03222011) from Sigma–Aldrich.

Acknowledgment

This work was supported by the European Research Training Network (MEBEL contract HPRN-CT-2002-00264).

References and notes

1. Ambler, R. P. *Philos. Trans. R. Soc. London, Ser. B* **1980**, *289*, 321–331.
2. Galleni, M.; Lamotte-Brasseur, J.; Rossolini, G. M.; Spencer, J.; Dideberg, O.; Frere, J. M. *Antimicrob. Agents Chemother.* **2001**, *45*, 660–663.
3. Garau, G.; Garcia-Saez, I.; Bebrone, C.; Anne, C.; Mercuri, P.; Galleni, M.; Frere, J. M.; Dideberg, O. *Antimicrob. Agents Chemother.* **2004**, *48*, 2347–2349.
4. Carfi, A.; Pares, S.; Duee, E.; Galleni, M.; Duez, C.; Frere, J. M.; Dideberg, O. *EMBO J.* **1995**, *14*, 4914–4921.
5. Carfi, A.; Duee, E.; Paul-Soto, R.; Galleni, M.; Frere, J. M.; Dideberg, O. *Acta Crystallogr. D* **1998**, *54*, 47–57.
6. Concha, N. O.; Rasmussen, B. A.; Bush, K.; Herzberg, O. *Structure* **1996**, *4*, 823–836.

7. Concha, N. O.; Rasmussen, B. A.; Bush, K.; Herzberg, O. *Protein Sci.* **1997**, *6*, 2671–2676.
8. Concha, N. O.; Janson, C. A.; Rowling, P.; Pearson, S.; Cheever, C. A.; Clarke, B. P.; Lewis, C.; Galleni, M.; Frere, J. M.; Payne, D. J.; Bateson, J. H.; Abdel-Meguid, S. S. *Biochemistry* **2000**, *39*, 4288–4298.
9. Fabiane, S. M.; Sohi, M. K.; Wan, T.; Payne, D. J.; Bateson, J. H.; Mitchell, T.; Sutton, B. J. *Biochemistry* **1998**, *37*, 12404–12411.
10. Fitzgerald, P. M. D.; Wu, J. K.; Toney, J. H. *Biochemistry* **1998**, *37*, 6791–6800.
11. Li, Z.; Rasmussen, B. A.; Herzberg, O. *Protein Sci.* **1999**, *8*, 249–252.
12. Payne, D. J.; Hueso-Rodriguez, J. A.; Boyd, H.; Concha, N. O.; Janson, C. A.; Gilpin, M.; Bateson, J. H.; Cheever, C.; Niconovich, N. L.; Pearson, S.; Rittenhouse, S.; Tew, D.; Diez, E.; Perez, P.; de la Fuente, J.; Rees, M.; Rivera-Sagredo, A. *Antimicrob. Agents Chemother.* **2002**, *46*, 1880–1886.
13. Toney, J. H.; Fitzgerald, P. M. D.; Grover-Sharma, N.; Olson, S. H.; May, W. J.; Sundelof, J. G.; Vanderwall, D. E.; Cleary, K. A.; Grant, S. K.; Wu, J. K.; Kozarich, J. W.; Pompliano, D. L.; Hammond, G. G. *Chem. Biol.* **1998**, *5*, 185–196.
14. Toney, J. H.; Hammond, G. G.; Fitzgerald, P. M. D.; Sharma, N.; Balkovec, J. M.; Rouen, G. P.; Olson, S. H.; Hammond, M. L.; Greenlee, M. L.; Gao, Y. D. *J. Biol. Chem.* **2001**, *276*, 31913–31918.
15. Garcia-Saez, I.; Hopkins, J.; Papamicael, C.; Franceschini, N.; Amicosante, G.; Rossolini, G. M.; Galleni, M.; Frere, J. M.; Dideberg, O. *J. Biol. Chem.* **2003**, *278*, 23868–23873.
16. Garau, G.; Bebrone, C.; Anne, C.; Galleni, M.; Frere, J. M.; Dideberg, O. *J. Mol. Biol.* **2005**, *345*, 785–795.
17. Garcia-Saez, I.; Mercuri, P. S.; Papamicael, C.; Kahn, R.; Frere, J. M.; Galleni, M.; Rossolini, G. M.; Dideberg, O. *J. Mol. Biol.* **2003**, *325*, 651–660.
18. Ullah, J. H.; Walsh, T. R.; Taylor, I. A.; Emery, D. C.; Verma, C. S.; Gamblin, S. J.; Spencer, J. *J. Mol. Biol.* **1998**, *284*, 125–136.
19. Paul-Soto, R.; Bauer, R.; Frere, J. M.; Galleni, M.; Meyer-Klaucke, W.; Nolting, H.; Rossolini, G. M.; de Seny, D.; Hernandez-Valladares, M.; Zeppezauer, M.; Adolph, H. W. *J. Biol. Chem.* **1999**, *274*, 13242–13249.
20. Heinz, U.; Adolph, H. W. *Cell. Mol. Life Sci.* **2004**, *61*, 2827–2839.
21. Walter, M. W.; Felici, A.; Galleni, M.; Soto, R. P.; Adlington, R. M.; Baldwin, J. E.; Frere, J. M.; Gololobov, M.; Schofield, C. J. *Bioorg. Med. Chem. Lett.* **1996**, *6*, 2455–2458.
22. Nagano, R.; Adachi, Y.; Imamura, H.; Yamada, K.; Hashizume, T.; Morishima, H. *Antimicrob. Agents Chemother.* **1999**, *43*, 2497–2503.
23. Zervosen, A.; Valladares, M. H.; Devreese, B.; Prosperi-Meys, C.; Adolph, H. W.; Mercuri, P. S.; Vanhove, M.; Amicosante, G.; Van Beeumen, J.; Frere, J. M.; Galleni, M. *Eur. J. Biochem.* **2001**, *268*, 3840–3850.
24. Venkatesan, A. M.; Gu, Y. S.; Dos Santos, O.; Abe, T.; Agarwal, A.; Yang, Y. J.; Petersen, P. J.; Weiss, W. J.; Mansour, T. S.; Nukaga, M.; Hujer, A. M.; Bonomo, R. A.; Knox, J. R. *J. Med. Chem.* **2004**, *47*, 6556–6568.
25. Walter, M. W.; Valladares, M. H.; Adlington, R. M.; Amicosante, G.; Baldwin, J. E.; Frere, J. M.; Galleni, M.; Rossolini, G. M.; Schofield, C. J. *Bioorg. Chem.* **1999**, *27*, 35–40.
26. Mollard, C.; Moali, C.; Papamicael, C.; Damblon, C.; Vessilier, S.; Amicosante, G.; Schofield, C. J.; Galleni, M.; Frere, J. M.; Roberts, G. C. K. *J. Biol. Chem.* **2001**, *276*, 45015–45023.
27. Siemann, S.; Clarke, A. J.; Viswanatha, T.; Dmitrienko, G. I. *Biochemistry* **2003**, *42*, 1673–1683.
28. Yang, K. W.; Crowder, M. W. *Arch. Biochem. Biophys.* **1999**, *368*, 1–6.
29. Bounaga, S.; Galleni, M.; Laws, A. P.; Page, M. I. *Bioorg. Med. Chem.* **2001**, *9*, 503–510.
30. Sanschagrin, F.; Levesque, R. C. *Antimicrob. Agents Chemother.* **2005**, *55*, 252–255.
31. Payne, D. J.; Bateson, J. H.; Gasson, B. C.; Proctor, D.; Khushi, T.; Farmer, T. H.; Tolson, D. A.; Bell, D.; Skett, P. W.; Marshall, A. C.; Reid, R.; Ghosez, L.; Combret, Y.; MarchandBrynaert, J. *Antimicrob. Agents Chemother.* **1997**, *41*, 135–140.
32. Heinz, U.; Bauer, R.; Wommer, S.; Meyer-Klaucke, W.; Papamicael, C.; Bateson, J.; Adolph, H. W. *J. Biol. Chem.* **2003**, *278*, 20659–20666.
33. Siemann, S.; Evanoff, D. P.; Marrone, L.; Clarke, A. J.; Viswanatha, T.; Dmitrienko, G. I. *Antimicrob. Agents Chemother.* **2002**, *46*, 2450–2457.
34. Olsen, L.; Pettersson, I.; Hemmingsen, L.; Adolph, H. W.; Jorgensen, F. S. *J. Comput. Aided Mol. Des.* **2004**, *18*, 287–302.
35. Wommer, S.; Rival, S.; Heinz, U.; Galleni, M.; Frere, J. M.; Franceschini, N.; Amicosante, G.; Rasmussen, B.; Bauer, R.; Adolph, H. W. *J. Biol. Chem.* **2002**, *277*, 24142–24147.
36. Hemmingsen, L.; Damblon, C.; Antony, J.; Jensen, N.; Adolph, H. W.; Wommer, S.; Roberts, G. C. K.; Bauer, R. *J. Am. Chem. Soc.* **2001**, *123*, 10329–10335.
37. Damblon, C.; Jensen, M.; Ababou, A.; Barsukov, I.; Papamicael, C.; Schofield, C. J.; Olsen, L.; Bauer, R.; Roberts, G. C. K. *J. Biol. Chem.* **2003**, *278*, 29240–29251.
38. Antony, J.; Gresh, N.; Olsen, L.; Hemmingsen, L.; Schofield, C. J.; Bauer, R. *J. Comput. Chem.* **2002**, *23*, 1281–1296.
39. Jones, G.; Willett, P.; Glen, R. C.; Leach, A. R.; Taylor, R. *J. Mol. Biol.* **1997**, *267*, 727–748.
40. Catalyst Version 4.6, Accelrys, San Diego, USA, <www.accelrys.com>.
41. Greene, J.; Kahn, S.; Savoj, H.; Sprague, P.; Teig, S. *J. Chem. Inf. Comput. Sci.* **1994**, *34*, 1297–1308.
42. Hahn, M. *J. Chem. Inf. Comput. Sci.* **1997**, *37*, 80–86.
43. Smellie, A.; Kahn, S. D.; Teig, S. L. *J. Chem. Inf. Comput. Sci.* **1995**, *35*, 285–294.
44. Smellie, A.; Kahn, S. D.; Teig, S. L. *J. Chem. Inf. Comput. Sci.* **1995**, *35*, 295–304.
45. Smellie, A.; Teig, S. L.; Towbin, P. *J. Comput. Chem.* **1995**, *16*, 171–187.
46. Sybyl molecular modelling software, Tripos, St. Louis, USA, <www.tripos.com>.
47. Simca-P, Version 10.0, Umetrics AB, Umeå, Sweden.